Article

18,18#-Dihexyl[9,9#]biphenanthro[9,10-*b*]triphenylene: Construction and Consequences of a Profoundly Hindered Aryl#Aryl Single Bond

Cameron L. Hilton, Jeremy M. Crowfoot, Pawel Rempala, and Benjamin T. King

J. Am. Chem. Soc., **2008**, 130 (40), 13392-13399 • DOI: 10.1021/ja803396n • Publication Date (Web): 10 September 2008

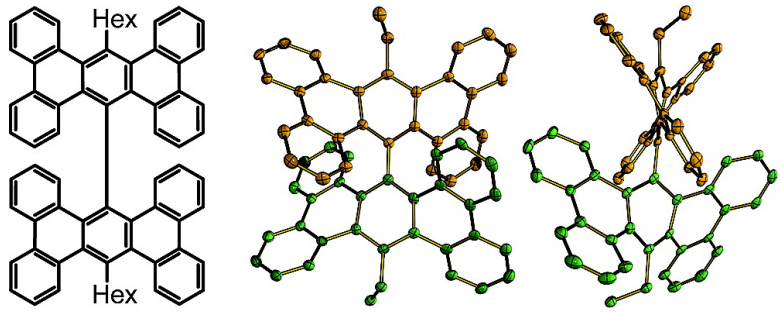

More About This Article

Additional resources and features associated with this article are available within the HTML version:

- Supporting Information
- Access to high resolution figures
- Links to articles and content related to this article
- Copyright permission to reproduce figures and/or text from this article

View the Full Text HTML

J|A|C|S
ARTICLES

Published on Web 09/10/2008

18,18′-Dihexyl[9,9′]biphenanthro[9,10-*b*]triphenylene: Construction and Consequences of a Profoundly Hindered Aryl−Aryl Single Bond

Cameron L. Hilton, Jeremy M. Crowfoot, Pawel Rempala, and Benjamin T. King*

Department of Chemistry, University of Nevada, Reno, Reno, Nevada 89557-0216

Received May 7, 2008; E-mail: king@chem.unr.edu

Abstract: The title compound, **1-Hex**, was synthesized by the Zr-mediated biphenylation of 4,4′-dihexyloctabromobiphenyl using $(Li(THF)_4)_2 \cdot Zr(biphe)_3$, where biphe is the 2,2′-biphenyldiyl ligand, in 5% isolated yield. Two independent X-ray diffraction analyses revealed that arene **1-Hex** possesses a highly strained and hindered aryl−aryl single bond. This bond causes the phenanthro[9,10-*b*]triphenylene (PTP) moieties to twist (anthracene subunit dihedral, 69°); the interlocked, helical, homochiral PTP moieties give rise to effective D_2 symmetry. The calculated adiabatic homolytic bond dissociation energy of this strained bond is only 67 kcal/mol, but nonetheless the bond exhibits a surprisingly normal length (1.49 Å); the reason is elongation only slowly releases strain. Variable temperature NMR revealed two dynamic processes: hexyl rotation (12.0 ± 0.4 kcal/mol) and inversion of chirality (15.2 ± 0.6 kcal/mol). DFT calculations provide rate-determining transitions states, whose energies agree with measured values, and provide insight to the mechanism of these processes. Rotation about the central bond is not involved in either observed process. Calculations demonstrate that rotation does not involve a simple torsion of the equilibrium structure, but rather a complex movement with a barrier of 49 kcal/mol from a slipped-parallel, C_{2h} intermediate.

Introduction

We report the synthesis, characterization, and conformational analysis of the title arene **1-Hex**, in which two phenanthro[9,10-*b*]triphenylene (PTP) moieties are joined through their sterically hindered 9 positions (Figure 1). This single bond joins two *gulfs*, a term we coin by extension of the established bay, cove, and fjord nomenclature[1] (Figure 1). Steric congestion twists the PTP moieties[2] and hinders rotation about the central bond, giving rise to rich conformational behavior.

Pascal's pioneering syntheses[2,3] of gulf-substituted PAHs were motivated by an interest in the relationship between steric congestion, reactivity, structure, and properties; the story is told in an engaging review.[4] Other gulf-substituted PAHs have been synthesized and studied due to their role in carcinogenesis.[5] PAHs bearing COOR′ (R′ = H, alkyl) in a gulf have been used as rigid spacers for molecular tweezers.[6,7]

The simplest PAH with a gulf architecture is dibenzo[*a*,*j*]anthracene (**2-H**, Figure 2); the placement of a substituent in the gulf region (position 14) introduces much strain and distorts the PAH skeleton from planarity. Its derivatives **2-COOH** and **2-COOR′** were used as a rigid spacer for molecular tweezers

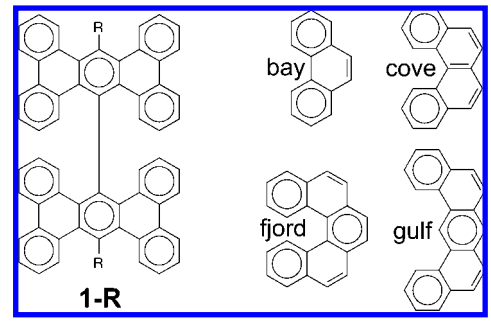

Figure 1. Structure of **1-R** and definitions of concave PAH regions.

and were prepared via a pyrylium salt.[6] The **2-Ph** derivative was recently prepared using a Wagner−Meerwein rearrangement of a substituted 9-fluorenylmethanol.[8] The second skeleton in this family, naphtho[1,2-*b*]triphenylene (**3-H**), bears an additional *ortho*-fused ring (Figure 2) but still has only one gulf. The derivative **3-Me** was synthesized by a Grignard route from the corresponding quinone,[9] and the derivative **3-Ph** was prepared by the Diels−Alder cycloaddition of phencyclone with 4-chlorodihydronaphthalene followed by oxidation.[10] The third skeleton, phenanthro[9,10-*b*]triphenylene (**4-H**), has two gulfs (Figure 2). Pascal and co-workers prepared its gulf-substituted derivatives **4-Ph** and **4-(*p*-C$_6$H$_4$X)** using a Diels−Alder approach, in which 9,10-didehydrophenanthrene reacts with phen-

(1) Fetzer, J. C. *Large (C ≥ 24) Polycyclic Aromatic Hydrocarbons: Chemistry and Analysis*; Wiley & Sons: New York, 2000; p 6.
(2) Pascal, R. A., Jr.; McMillan, W. D.; Van Engen, D. *J. Am. Chem. Soc.* **1986**, *108*, 5652–5653.
(3) Pascal, R. A., Jr.; McMillan, W. D.; Van Engen, D.; Eason, R. G. *J. Am. Chem. Soc.* **1987**, *109*, 4660–4665.
(4) Pascal, R. A., Jr *Pure Appl. Chem.* **1993**, *65*, 105–110.
(5) Gill, R. D.; Beltran, L.; Nettikumara, A. N.; Harvey, R. G.; Koostra, A.; DiGiovanni, J. *Mol. Carcinog.* **1992**, *6*, 53–59.
(6) Zimmerman, S. C. *Tetrahedron Lett.* **1988**, *29*, 983–986.
(7) Zimmerman, S. C.; Zeng, Z.; Wu, W.; Reichert, D. E. *J. Am. Chem. Soc.* **1991**, *113*, 183–196.
(8) Yang, Y.; Dai, W.; Zhang, Y.; Petersen, J. L.; Wang, K. K. *Tetrahedron* **2006**, *62*, 4364–4371.
(9) Lambert, P.; Martin, R. H. *Bull. Soc. Chim. Belg.* **1952**, *61*, 513–523.
(10) Mondal, S.; Bandyopadhyay, K.; Bhattacharya, A. J. *Curr. Sci.* **1985**, *54*, 455–458.

10.1021/ja803396n CCC: $40.75

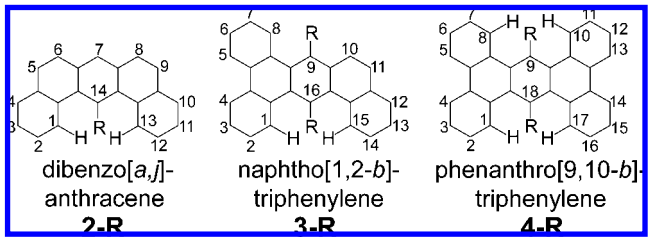

Figure 2. Some known PAHs with gulfs. Unsaturation and nongulf H atoms are omitted for clarity.

Scheme 1. Synthesis of **1-Hex**

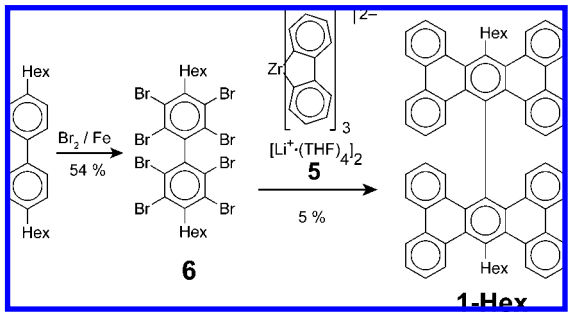

cyclone dienes, or by the pyrolysis of phencyclone dienes.[2,3] Rabinovitz and co-workers developed another route to **4-Ph**, the Li-mediated coupling and subsequent oxidation of hexaphenylbenzene.[11] The last method for the preparation of this skeleton is the 2-fold, Zr-mediated biphenylation of 1,4-disubstituted tetrabromobenzene, which we previously employed for the preparation of **4-Me**.[12] We also use this method for the synthesis of **1-Hex.**

1-Hex is unique—it is the only known compound with a gulf−gulf bond. This structural element gives rise to several phenomena that merit investigation. It introduces a great deal of strain, but the 9,9′ bond exhibits a paradoxically normal length. It gives rise to a chiral equilibrium structure and rich conformational dynamics. Sterics profoundly hinder rotation about the 9,9′ bond.

Results and Discussion

Synthesis. The synthesis of **1-Hex** uses the recently developed reagent $(Li(THF)_4)_2 \cdot Zr(biphe)_3$ (**5**, biphe is 2,2′-biphenyldiyl)[13] to effect the 4-fold biphenylation of 4,4′-dihexyloctabromobiphenyl (**6**). The basic reaction is a double *ipso* substitution on an *ortho*-dihaloarene to form a triphenylene fragment.[12] To the best of our knowledge, the only other method for this transformation is the recently reported Stille coupling with a 2,2′-distannylbinaphthyl reagent under microwave irradiation.[14]

Exhaustive electrophilic bromination of 4,4′-dihexylbiphenyl, which was prepared by Kumada coupling of 4,4′-dibromobiphenyl with hexylmagnesium bromide, gives octabromide **6**. Treatment of **6** with **5** afforded **1-Hex** in 5% isolated yield (Scheme 1). Byproducts, which are mostly oligophenyls, were removed by trituration with hexane. Preparative HPLC (silica gel, hexane/chloroform) followed by crystallization from benzene gave pure **1-Hex**. This compound can be stored in air and

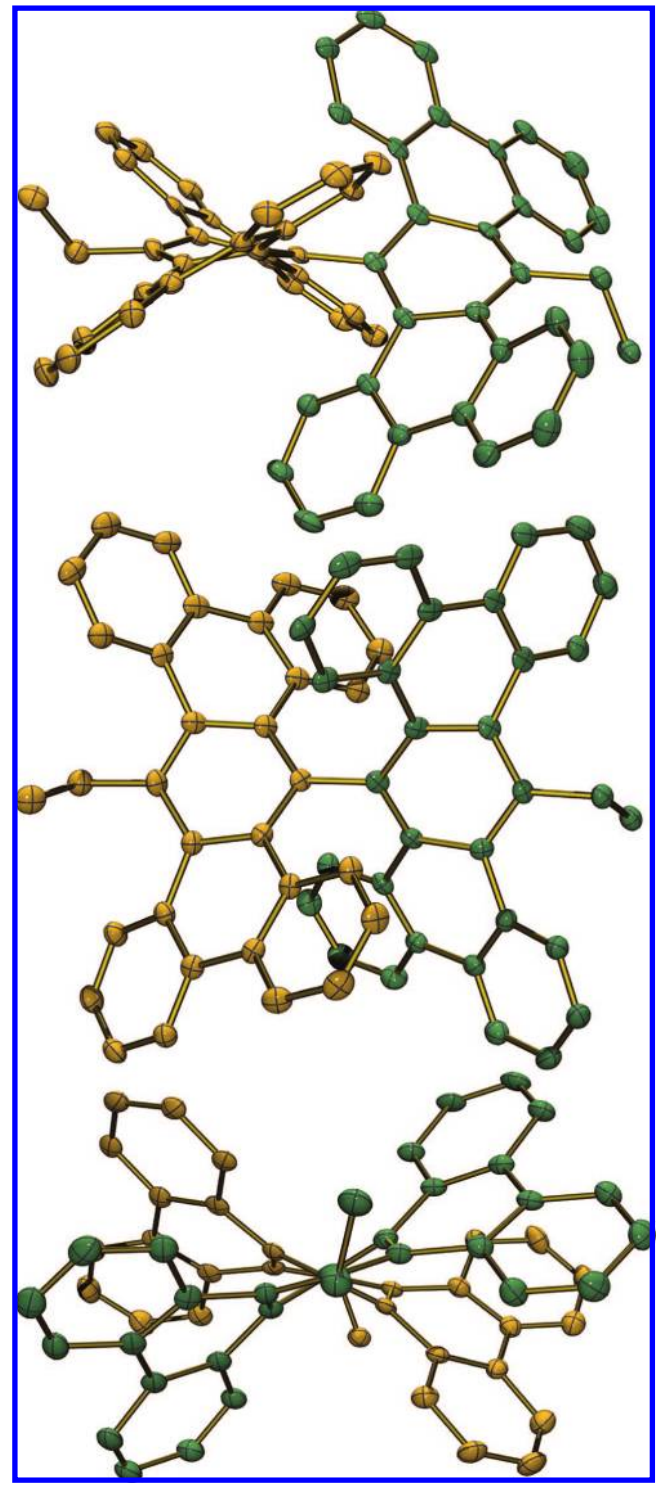

Figure 3. Three views of the X-ray diffraction analysis structure of **1-Hex**•$(benzene)_{0.5}$. Hydrogen atoms, solvent, and the terminal four carbon atoms of the hexyl groups are omitted for clarity.

is soluble in THF, toluene, benzene, chloroform, and dichloromethane. No light sensitivity has been noted.

Static Structure. The structure of **1-Hex** was determined by two independent single crystal X-ray diffraction analyses.[15] While the crystals differed in the number of benzene solvate molecules and in the conformations of the hexyl chains, the geometries of the PAH cores were nearly identical.

Three perspectives of one structure, the hemisolvate, are shown in Figure 3. The PTP moieties twist, in the same chiral

(11) Eshdat, L.; Ayalon, A.; Beust, R.; Shenhar, R.; Rabinovitz, M. *J. Am. Chem. Soc.* **2000**, *122*, 12637–12645.
(12) Hilton, C. L.; Jamison, C. R.; King, B. T. *J. Am. Chem. Soc.* **2006**, *128*, 14824–14824.
(13) Hilton, C. L.; King, B. T. *Organometallics* **2006**, *25*, 4058–4061.
(14) Xue, X.; Scott, L. T. *Org. Lett.* **2007**, *9*, 3937–3940.

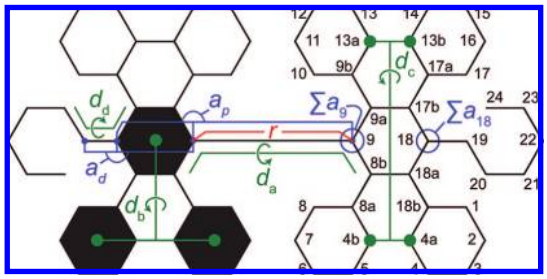

Figure 4. Numbering and characteristic metrics of **1-Hex**.

Table 1. Measurements of **1-Hex**

geometry	r/Å	d_a, σ/deg, n^a	d_b, σ/deg, n^a	d_c, σ/deg, n^a
X-ray, disolvate[b]	1.490(2)	57.8, 1.9, 2	36.7, 1.6, 4	69.2, 2.2, 2
X-ray, hemisolvate[b]	1.487(3)	57.8, 2.1, 2	36.5, 1.6, 4	69.0, 3.0, 2
B3LYP/6-31G(d)[c]	1.500	54.6, 0.4, 2	38.8, 0.4, 4	74.6, 0.0, 2
HF/6-31G(d)[d]	1.505	54.3, 0, 1	39.5, 0.2, 2	75.5, 0, 1
PM3[d]	1.480	57.8, 0, 1	38.3, 0.2, 2	71.8, 0, 1
AMBER[d,e]	1.484	42.6, 0, 1	39.9, 0.1, 2	74.9, 0, 1

[a] Number of measurements. [b] No molecular symmetry. [c] No molecular symmetry, close to C_2 point group, hexyl groups all *anti*. [d] C_2 point group. [e] Modified AMBER force field.

Scheme 2. Homodesmotic Strain Energies (B3LYP/6-31G(d), ΔE_{el}, ΔG_{298} in parentheses) for **1-Me**

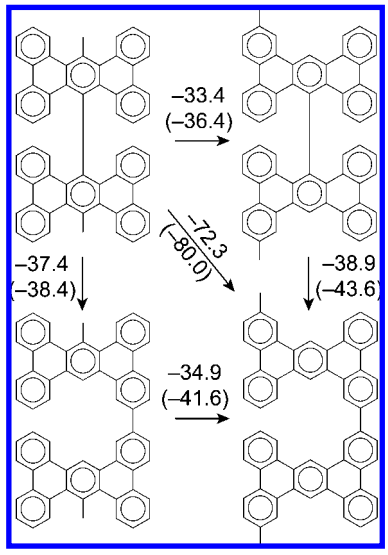

sense, to accommodate one another. The resulting structure is reminiscent of a handshake, a term we employ as a trivial name. Several metrics (Figure 4) describe the static geometry: the length of the central bond r, the dihedral angle d_a about the central bond (8b, 9, 9′, 8b′), and the dihedral angle describing the twist of a PTP moiety. Two definitions of this twist dihedral are used in the literature: (1) the angle d_b between the least-squares plane of the central ring and the least-squares plane of the two distal rings[16] and (2) the angle d_c, which is the greater of the dihedral 4a, 4b, 13a, 13b or dihedral 4b, 4a, 13b, 13a.[17] To facilitate comparisons, we report values for both definitions in Table 1. The other metrics d_d, a_p, a_d, Σa_9, and Σa_{18} are needed to describe dynamic behavior and will be discussed later.

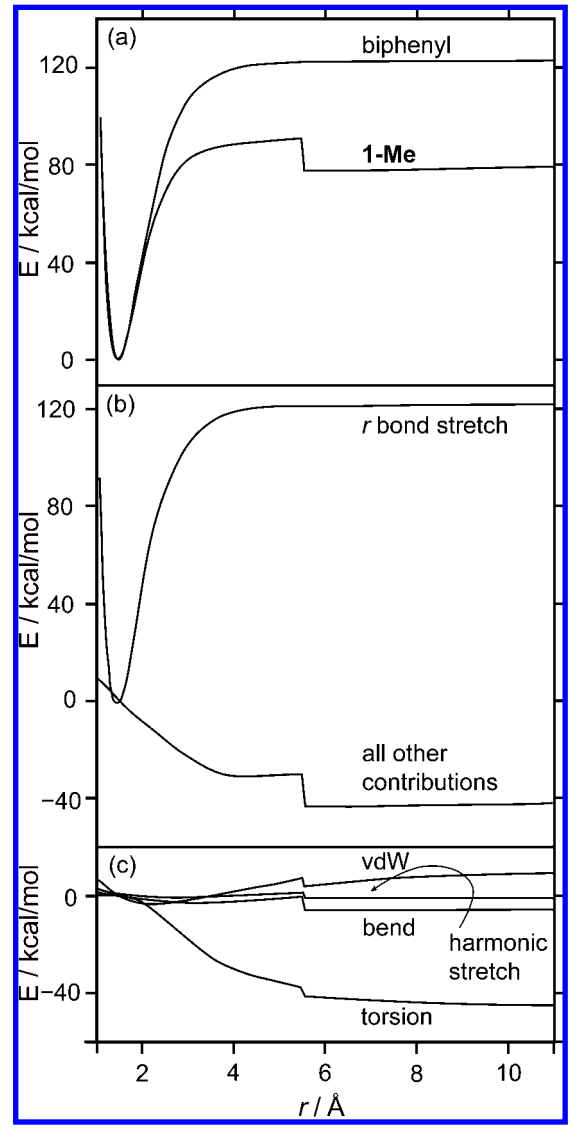

Figure 5. AMBER energies as a function of r. (a) Bond dissociation for **1-Me** and biphenyl. (b) Partitioning of the dissociation energy of **1-Me** into the Morse stretch of the central bond and all other contributions. (c) Partition of all other contributions for **1-Me** (except the improper dihedral term, which is small and nearly constant). In (b) and (c), all partition curves were set to 0 kcal/mol at the equilibrium distance.

The X-ray diffraction data reveal a surprisingly ordinary central bond length r, 1.49 Å (cf. 9,9′-bianthracene,[18] 1.50 Å), despite the large amount of strain in this hindered central bond (see below). The dihedral angle d_a is 57.8° (cf. 9,9′-bianthracene,[18] 79.1°). The PTP moieties are highly twisted, with an average torsion angle d_c of 69° (cf. **4-Ph**,[3] 66°), but less than that of the current record holder, hexaphenyltetrabenzo[*a*,*c*,*l*,*n*]pentacene, in which an anthracene subunit exhibits a twist of 86°.[19]

(15) Disolvate: $C_{84}H_{70}$ ($C_{72}H_{58}\cdot(C_6H_6)_2$); FW 1079.40; triclinic; $P\bar{1}$; pale yellow; a = 8.98780(10) Å; b = 15.3483(2) Å; c = 21.4148(3) Å; α = 86.2720(10)°; β = 89.2610(10)°; γ = 78.7930(10)°; cell volume = 2891.65(6) Å^3; temp 100 K; Z = 2; R = 0.038; GOF = 1.09. Hemisolvate: $C_{75}H_{61}$ ($C_{72}H_{58}\cdot(C_6H_6)_{0.5}$); FW = 962.24; triclinic; $P\bar{1}$; pale yellow; a = 8.9148(15) Å; b = 13.982(2) Å; c = 21.420(4) Å; α = 104.888(3)°; β = 96.430(3)°; γ = 94.489(3)°; cell volume = 2548.0(7) Å^3; temp 100 K; Z = 2; R = 0.054; GOF = 0.92.

(16) Barnett, L.; Ho, D. M.; Baldridge, K. K.; Pascal, R. A., Jr *J. Am. Chem. Soc.* **1999**, *121*, 727–733.
(17) Pascal, R. A., Jr *Chem. Rev* **2006**, *106*, 4809–4819.
(18) Kyziol, J. B.; Zaleski, J. *Acta Crystallogr., Sect. E* **2007**, *63*, o1235.
(19) Lu, J.; Ho, D. M.; Vogelaar, N. J.; Kraml, C. M.; Bernhard, S.; Byrne, N.; Kim, L. R.; Pascal, R. A., Jr *J. Am. Chem. Soc.* **2006**, *128*, 17043–17050.

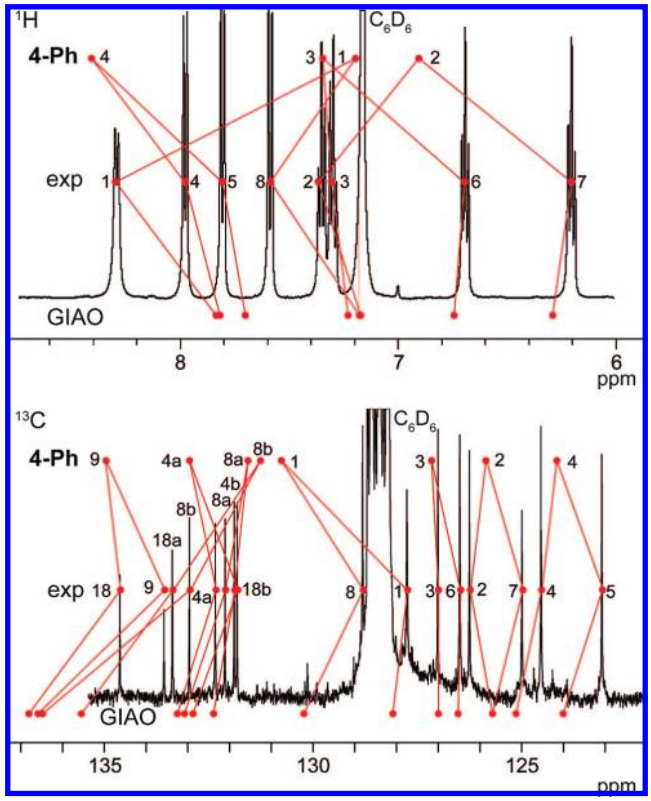

Figure 6. Aryl regions of the ^{1}H and ^{13}C NMR spectra of **1-Hex** (C_6D_6) (black); correlation of the chemical shifts of **4-Ph** with the calculated (GIAO-B3LYP/6-31G(d)) and experimental chemical shifts of **1-Hex** (red).

Scheme 3. Dynamic Processes in **1-Hex**

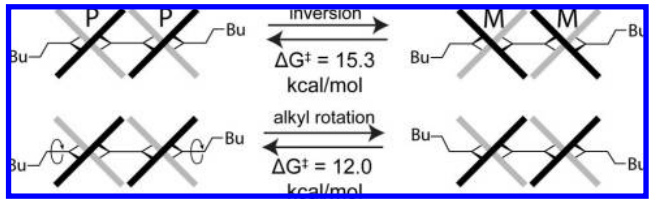

Computational methods (B3LYP/6-31G(d), PM3, and a customized AMBER force field (see Supporting Information)) adequately reproduce experimental geometries (Table 1). The greatest discrepancy is the small dihedral angle d_a obtained using the AMBER model, which brings the PTP blades artificially close. The HF bond length r for **1-Hex** is overestimated, despite the model's systematic underestimation of bond lengths.[20]

In many instances, we performed computational analyses on the analogues **1-Me**, **1-Et**, and **1-H** to simplify the location of stationary points by reducing the number of alkyl conformations. Compound **1-Me** served for estimation of strain and rotation about the central bond; **1-Et** was used to elucidate details of alkyl motion, and the high symmetry of **1-H** enabled quick calculation of NMR chemical shifts for benchmarking.

Strain. The homodesmotic reactions of Scheme 2 can be used to define the strain energy arising from connectivity in gulf regions of **1-Me**. At the B3LYP/6-31G(d) level, the gulf methyl groups introduce ~34 kcal/mol of strain, and the central bond introduces ~38 kcal/mol of strain. These strain energies are not entirely independent; their values depend on the order in which the functionality is removed from the gulf; we report the average. The methyl contribution compares remarkably well with the

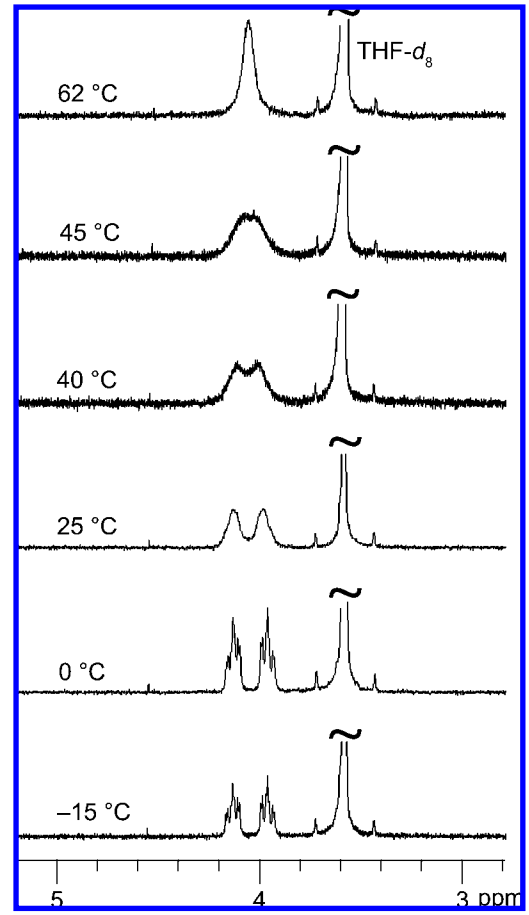

Figure 7. Variable temperature ^{1}H NMR spectra (500 MHz, THF-d_8) showing CH_2(19) of **1-Hex**.

strain of **4-Me**.[12]Because the hexyl groups in **1-Hex** can be arranged in a way that does not present additional steric demand, the strain energy of **1-Hex** should be nearly identical to that for **1-Me**, 72 kcal/mol. Other methods give similar total strain energies: PM3, 64.8 kcal/mol; AM1, 58.1; AMBER, 61.0; and SYBYL, 75.3. MMFF94 performs poorly, giving 115.4 kcal/mol.

Bond Energy. The central bond in **1-R** introduces a great deal of strain, suggesting that it is weak. Indeed, it is: the homolytic bond dissociation energy (ΔG_{298}, HBDE, B3LYP/6-31G(d)) of **1-Me** is 102.5 kcal/mol (vertical) and 68.3 kcal/mol (adiabatic). The relaxation energy (34.2 kcal/mol) is close to the strain manifest in the central bond (37.4 kcal/mol). At the same level of theory, the HBDE of biphenyl is 121.0 kcal/mol (vertical) and 115.2 kcal/mol (adiabatic); the experimental (ΔH_{298}) value is 118.9 ± 1.4 kcal/mol.[21] The adiabatic HBDE of **1-R** is only ~55% of that in biphenyl.

Bond Length. The length of the central bond in **1-Hex** (1.490 Å) is essentially identical to that of biphenyls without substitution *ortho* to the central bond (1.487 Å, σ = 0.007 Å) and

(20) Hehre, W. J. *A Guide to Molecular Mechanics and Quantum Mechanical Calculations*; Wavefunction Inc.: Irvine, CA, 2003; p 94.
(21) (a) Chirico, R. D.; Knipmeyer, S. E.; Nguyen, A.; Steele, W. V. *J. Chem. Thermodyn.* **1989**, *21*, 1307–1331. (b) Davico, G. E.; Bierbaum, V. M.; DePuy, C. H.; Ellison, G. B.; Squires, R. R. *J. Am. Chem. Soc.* **1995**, *117*, 2590–2599.
(22) Allen, F.; Kennard, O.; Watson, D. G.; Brammer, L.; Orpen, A. G.; Taylor, R. *J. Chem. Soc., Perkin Trans.* **1987**, *2*, S1.

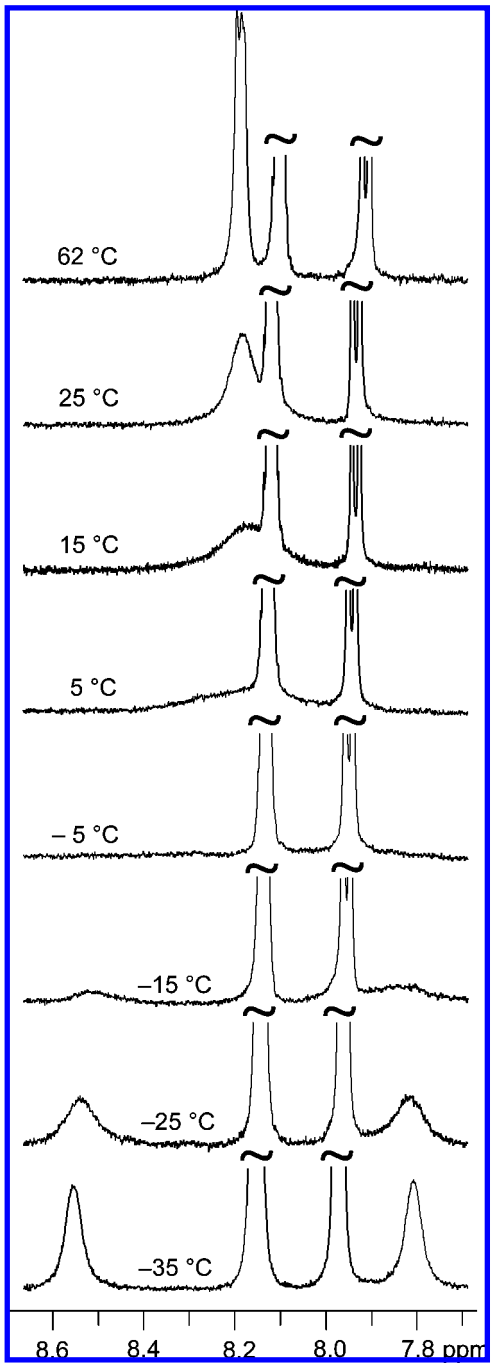

Figure 8. Variable temperature ^{1}H NMR spectra (500 MHz, THF-d_8) showing CH(1) and CH(17) of **1-Hex**.

biphenyls with subsitution *ortho* to the central bond (1.490 Å, $\sigma = 0.010$ Å).[22] Why does the weak central bond of **1-Hex**, which has only 55% of the normal strength of a biphenyl central bond, exhibit a normal bond length? We address this question by exploring the potential energy surface of **1-Me** at intermediate bond lengths, stretching the central bond from equilibrium to 11 Å. This problem is computationally challenging because the wave function is multideterminant within this bond length range, which makes any realistic electronic structure calculation unaffordable for this large molecule.

Fortunately, molecular mechanics methods are suitable;[23] this is because we are interested in the relationship between energy

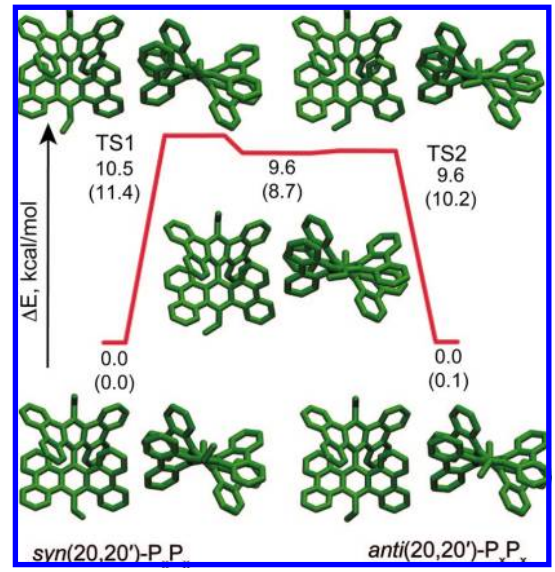

Figure 9. Low energy pathway for ethyl rotation in **1-Et** (B3LYP/6-31G(d)). Energies (ΔE, (ΔG)) are given in kcal/mol.

and geometry, not electronic structure. We customized the AMBER implementation in Gaussian 03 suite of programs to use a Morse potential for the aryl−aryl bond stretch, fitted to experimental data for biphenyl, instead of the normal harmonic potential. The potential energy curve for **1-Me** is shown below (Figure 5a), with that of biphenyl provided for comparison. The sudden release of strain energy (13.7 kcal/mol) at 5.5 Å, the point at which the PTP moieties disengage, is striking. Below 5.5 Å, strain is released gradually with extension. These observations provide insight to the normal equilibrium bond length for this weak bond.

Force, not energy, determines the equilibrium bond length: at equilibrium, the net force is zero. If the change of strain energy is small around the equilibrium geometry, then strain will not alter the equilibrium distance. This is the case for **1-R**, as shown by the decomposition of the AMBER energy (Figure 5).

Partitioning the dissociation energy into the Morse contribution and other contributions (Figure 5b) provides a quantitative but simple explanation of how these contributions affect bond length. We approximate the Morse curve as a harmonic potential with a force constant of 367 kcal/(mol Å^2) and a minimum at 1.46 Å, a value taken from the r bond stretch curve. We approximate all other contributions as a linear function with slope −17.5 kcal/(mol Å). This treatment provides an expected equilibrium bond length of 1.508 Å, slightly more than the calculated length of 1.484 Å. The reason that this weak bond has a normal length is that strain is relieved only slowly with dissociation.

Complete decomposition of energy (Figure 5c) reveals that most of the strain is torsional. At short distances, some van der Waals stabilization from the intramolecular attraction of the PTP moieties is evident.

The bond dissociation potential can be considered from the other direction: radical recombination. The step at ~5.5 Å, where the two PTP moieties just meet, is a significant (13.7 kcal/mol) barrier to recombination. Steric barriers to radical recombination are rare but have been described for the di-*tert*-butylated methyl radical.[23,24]

NMR Spectra. All ^{1}H and ^{13}C NMR resonances have been assigned (Figure 6) by a combination of DQF-COSY, NOE,

(23) Peyman, A.; Beckhaus, H.-D. *J. Comput. Chem.* **1992**, *13*, 541–550.

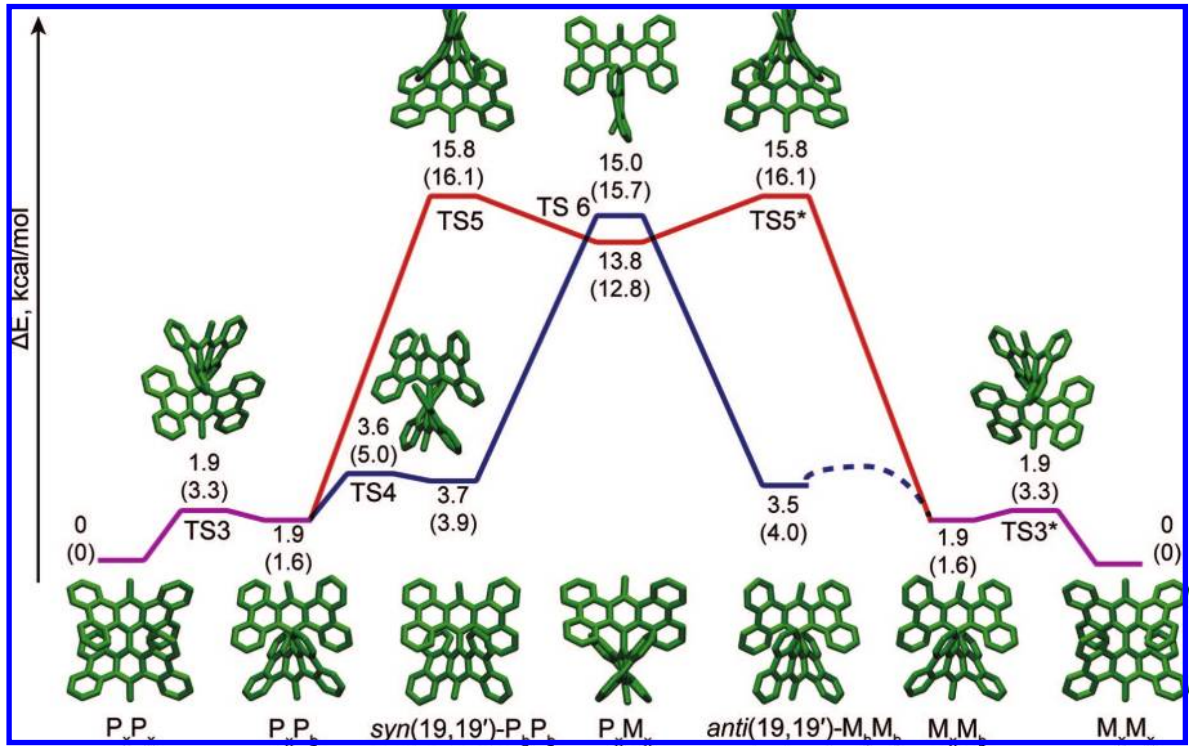

Figure 10. Low energy pathways for inversion of **1-Me** (B3LYP/6-31G(d)). Energies (ΔE, (ΔG)) are given in kcal/mol.

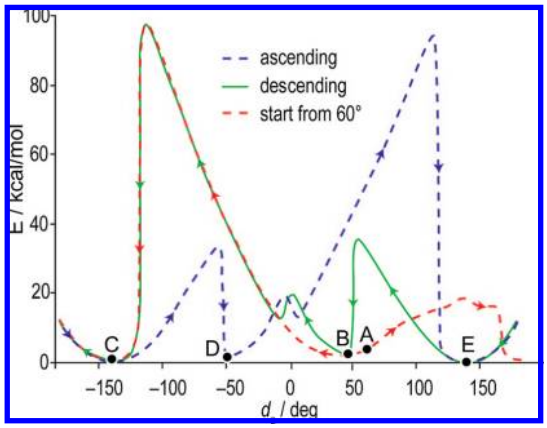

Figure 11. Relaxed energy scan of dihedral angle d_a in **1-Me** (AMBER).

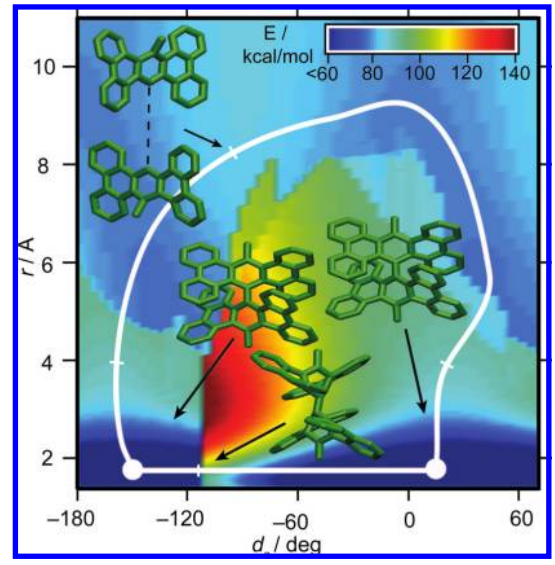

Figure 12. Relaxed PES for rotation and dissociation. Rotation (white, horizontal) and rotation/dissociation (white, curved) are shown.

HMQC, and HMBC spectra (see Supporting Information). GIAO NMR calculations support the assignments. Benchmark calculations were performed on the model system **1-H** at D_2 symmetry, using HF, B3LYP, OPBE, and PBEPBE functionals with 6-31G(d) and EPR-II basis sets (GIAO calculations) with the B3LYP/6-31G(d) geometry. Because all models predicted similar chemical shifts, we decided to use the more affordable B3LYP/6-31G(d)-GIAO//B3LYP/6-31G(d) level for NMR prediction of **1-Hex**. Indeed, the error introduced by not averaging the thermally accessible conformations probably outweighs the uncertainty of the DFT chemical shifts.

The calculated chemical shifts of the aryl resonances agree well, with root-mean-square (rms) deviations of 0.24 ppm (^{1}H) and 1.6 ppm (^{13}C). The ordering of the ^{1}H resonances is reproduced well, with only H(3) misordered. Theory is least accurate for the gulf-facing protons H(1) and H(8), with mean unsigned errors of 0.44 ppm. The ordering of the aryl ^{13}C resonances is also reproduced well, with only C(18a) and C(18b) misordered. The calculated ^{13}C resonances of the central ring of PTP (8b, 9, 18, 18a) have greater error (rms deviation, 2.8 ppm) than the other aromatic carbon sets (rms deviation, 0.7 ppm).

Comparison of the NMR spectra of **1-Hex** with **4-Ph**[11] is informative. Unsymmetrical substitution of the PTP moieties in **1-Hex** splits the resonances found in symmetrically substituted **4-Ph**; these correlations are traced in Figure 6. Protons facing the aryl gulf (6, 7, 8) are upfield of protons facing the aliphatic gulf. This is reasonable, as the aryl gulf-facing protons

(24) Rüchardt, C.; Backhaus, H.-D. *Top. Curr. Chem.* **1986**, *130*, S1.

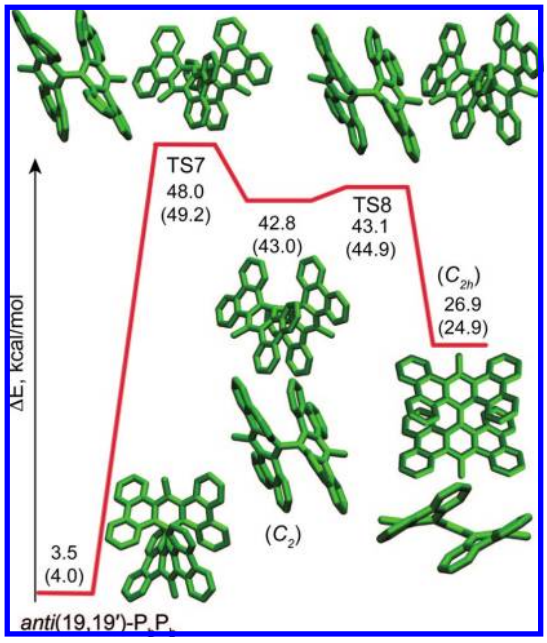

Figure 13. Low energy pathway for rotation about the central bond in **1-Me** (B3LYP/6-31G(d)). Energies (ΔE, (ΔG)) are given in kcal/mol.

experience a diatropic shift due to their proximity to the other PTP moiety. In the ^{13}C spectrum of **1-Hex** (and **4-Ph**), aryl carbons bearing protons are upfield of internal C atoms.

Variable Temperature NMR. Variable temperature (VT) ^1H NMR spectroscopy revealed two dynamic processes (Scheme 3). Inversion of chirality causes the diastereotopic protons of $CH_2(19)$ and $CH_2(20)$ to coalesce at 45 and 50 °C, respectively. Analysis of the coalescence of the $CH_2(19)$ resonances gives $\Delta G^{\ddagger}_{\text{inversion}}$ of 15.3 ± 0.5 kcal/mol, and analysis of the coalescence of resonances of $CH_2(20)$, which are partially obscured by solvent, gives a $\Delta G^{\ddagger}_{\text{inversion}}$ of 15.2 ± 0.6 kcal/mol (Figure 7). Pascal and co-workers reported a similar barrier to inversion, 16.7 kcal/mol, in **4-(*p*-*i*-PrC$_6$H$_4$)**.[3]

Hindered rotation of the hexyl groups about dihedral d_d lowers the apparent symmetry of the molecule from D_2 to C_2 (or C_1, depending on the relative orientations of the two of d_d dihedrals). Aryl protons H(1) and H(17) coalesce at −5 °C, giving a $\Delta G^{\ddagger}$ of 12.0 ± 0.4 kcal/mol. In addition, both pairs, H(8), H(10) and H(7), H(11), coalesce at −28 °C, giving a $\Delta G^{\ddagger}$ of 12.0 ± 0.5 kcal/mol (Figure 8). The barrier to alkyl group rotation in **1-Hex** is 12.0 ± 0.4 kcal/mol.

Optical Properties. The UV/vis spectrum of **1-Hex** (λ_{max} 311.5 nm) is similar to that of 9,18-dimethylphenanthro[9,10-*b*]triphenylene, **4-Me** (λ_{max} 313 nm). The emission spectrum (λ_{ex} 341 nm) exhibits a maximum at 480 nm, which represents a significant Stokes shift when compared to the emission maximum for **4-H** (λ_{ex} 335 nm, $\lambda_{max\ em}$ 381.5 nm).[25] This large Stokes shift could arise from the formation of an intramolecular exciplex or from the twist of the PTP moieties. Comparison with the fluorescence spectrum of **4-Ph** should resolve this question, but this spectrum apparently has not been reported.

Dynamics: Alkyl Rotation. Crystallography establishes the existence of hexyl group rotomers with similar energies. The two crystal structures of **1-Hex** differ in the orientation of alkyls about the 20−19−19′−20′ dihedral: in the hemisolvate, the alkyl groups are *anti*; in the disolvate, they are *syn*. To avoid confusion with a coincident dihedral relevant to inversion of chirality, we use the labels *syn*(20−20′) and *anti*(20−20′). We use the ethyl analogue, **1-Et**, the smallest model illustrating alkyl rotation, for our computational studies. Preliminary scans (PM3) about dihedral angle d_d revealed seven minima and nine transition states. These stationary points, when ordered according to d_d and connected, do not result in a physically reasonable sequence, but rather they constitute three independent pathways. The lowest of these pathways was investigated using the B3LYP/6-31G(d) model chemistry (Figure 9).

Calculations reveal that the conformers *syn*(20−20′) and *anti*(20−20′)-**1-Et** have essentially identical energies, in agreement with the observation that both conformers of **1-Hex** crystallize from benzene solution. The calculated barrier ($\Delta G^{\ddagger}$) for interconversion of these conformers, TS1, is 11.4 kcal/mol, in reasonable agreement with the barrier measured for **1-Hex**, 12.0 ± 0.5 kcal/mol.

Dynamics: Inversion of Chirality. Crystallography has established that low energy conformers of **1-Hex** are chiral. Variable temperature NMR has revealed a process, which we ascribe to chiral inversion (see below), with a barrier of $\Delta G^{\ddagger}$ = 15.2 ± 0.5 kcal/mol. What is the mechanism of inversion? As before, we address this question using calculations, here with the B3LYP 6-31G(d) model chemistry and the analogue **1-Me** (Figure 10).[26]

Several intermediates are involved, and their geometry must be defined. The helicity of each of their PTP moieties must be specified. We use the standard M/P descriptors. The orientation of the alkyl substituents, which can pop out of their congested axial positions, must also be specified. We use the descriptors "x" for axial and "b" for bent. If both alkyl groups are bent, then dihedral angle 19−18−18′−19′ is defined, with *syn*(19,19′) and *anti*(19,19′) conformations possible. The lowest energy calculated structure of **1-Me**, M_xM_x/P_xP_x, matches the crystallographic structures.

We have identified both stepwise and concerted pathways for inversion. In both cases, the sterically encumbering Me groups move out of their axial positions in the gulf to a bent position above the plane of the central ring of the PTP moiety. This movement is required because the gulf rings cannot easily pass one another with a methyl group in the axial position.

In the stepwise path, one methyl group moves out of the axial position to give P_xP_b, and then the helical PTP moiety inverts and its methyl group returns to its axial position (P_xM_x) via the rate-determining transition state TS5. The conformation P_xM_x is a high-energy, quasi-*meso* intermediate.

In the concerted path, both methyl groups move out of the plane, to give *syn*- or *anti*-P_bP_b. Both PTP moieties simultaneously invert in rate-determining transition state TS6. Curiously, TS6 connects the *syn*(19,19′) and the *anti* (19,19′) configurations; a methyl group is brought around with inversion of one of the PTP blades.

The structural changes associated with the movement of the Me groups from the gulfs are broadly distributed throughout the PTP moiety. The distal bend a_d (Figure 4) is 163° and the sum of bond angles at *ipso* C18, Σa_{18}, is 359°, demonstrating that the bend does not arise from changes in hybridization at the *ipso* C atom, but rather a distributed perturbation of torsion angles throughout the PTP moiety.

The rate-determining transition states of each pathway for the inversion of **1-Me** are comparably high in energy: stepwise,

(25) Colmsjö, A. L. *Anal. Chim. Acta* **1987**, *197*, 71–75.
(26) The modified Amber model chemistry also would have been appropriate, but transition states were more difficult to locate.

$\Delta G^{\ddagger}_{298}$ = 16.1 kcal/mol; concerted, $\Delta G^{\ddagger}_{298}$ = 15.7 kcal/mol. Both values are consistent with the barrier to inversion of 15.2 ± 0.5 kcal/mol for **1-Hex** determined by VT NMR. It should be noted that the racemization pathways involve only changes in helicity or the position of an alkyl group. Rotation about the central bond is not involved in either path.

Dynamics: Rotation about the Central Bond. Hindered rotation around a single σ bond is a central theme in stereochemistry. Although the origin of the internal rotation barrier in ethane is the subject of a recent debate,[27] it is obvious that the high rotational barriers of many substituted biaryls arise due to steric interactions. One of the most hindered biaryls that has been studied computationally and reported in literature is 9,9′-bianthracene, with a computed barrier to rotation of 39.7 kcal/mol (MP2/6-31G(d)//HF/3-21G).[28] The experimental barrier to racemization of 2,2′-dimethyl-1,1′-binaphthalene is 49.5 kcal/mol,[29] and the experimental barrier ($\Delta G^{\ddagger}$) for rotation of 2,2′,3,5′,6-pentachlorobiphenyl is 45.2 kcal/mol at 300 °C.[30] The lower bound for the barrier found in 2,2′,3,3′,6,6′-hexachlorobiphenyl is 50 kcal/mol at 320 °C.[30] The rotational barrier for decachlorobiphenyl, estimated as the energy difference (at B3LYP/6-311+G(d)) between the planar and optimal structure, is high, 135 kcal/mol.[31] As we will see below, this estimate is only a rough upper bound.

We first calculated (AMBER) the rotation about the 9,9′ bond of **1-Me** using the simple (and, as later described, inadequate) concept of a torsional potential about d_a (Figure 11). Initially, geometry **A** with $d_a = 60°$ was produced by distortion of the M_xM_x minimum. The dihedral was decreased (red curve), passing through the M_xM_x minimum **B**. Next, the energy rose sharply and fell abruptly to minimum **C**, which is structurally identical to **B**. Driving the torsion in the opposite sense gives a different behavior. Increasing the dihedral from −180° (blue curve), the M_xM_x minimum **C** is reached smoothly. An abrupt change then occurs: the Me groups pop out of the gulf, changing the geometry to *anti*(19,19′)P_bP_b, which descends to point **D**. Continuing to drive the torsion, **D** connects to P_xP_x minimum **E**.

Rotation about the central aryl−aryl bond is not just topologically strange—it is also chemically strange. The apparent barrier to rotation exceeds 90 kcal/mol (Figure 5), but the HBDE is only 67 kcal/mol! This suggests that dissociation into two radical fragments, rotation, and then recombination might provide a lower energy pathway to rotation. We examined this possibility by constructing a relaxed 2-D PES by scanning r and the dihedral angle d_a using the modified AMBER force field (Figure 12). Indeed, dissociation and recombination are competitive with simple rotation about d_a.

The hysteresis in the rotation about d_a in **1-Me** indicates that this torsion is a poor approximation of the rotational pathway. The torsion function is not single-valued and therefore is not a trajectory on the Born−Oppenheimer potential energy surface. Cioslowski has described these and other serious shortcomings of one-dimensional torsional potentials for molecules exhibiting hindered rotation.[32] The authors emphasized that such anomalous behavior is not a violation of microscopic reversibility, but rather that internal rotations often cannot be treated as a one-dimensional problem. Torsional potentials may also fail to describe motion in other geared, rotating systems, including some molecular motors.[32]

The mechanism of rotation can be properly described by the normal approach of locating transition states connecting minima. We returned to the B3LYP/631G(d) model chemistry. Because the interlocking of the PTP moieties was responsible for the high barrier in the scan of the torsional potential, we reasoned that a conformation where the PTP moieties were parallel and disengaged might possess a lower barrier to rotation.

The discovery of the disengaged conformation with C_{2h} symmetry satisfied our expectations (Figure 13). This conformation lies 26.9 kcal/mol above the P_xP_x global minimum. In this conformation, proximal C(9) and its symmetry equivalent C(9′) retain their sp^2 geometry, as evidenced by the sum of the bond angles about C(9) $\Sigma a_9 = 360°$ (Figure 4). The proximal bend a_p is 159°. The disengaged geometry is made possible by torsional distortions distributed through the PTP moieties, not localized changes in hybridization at C(9) and C(9′). From this conformation, the rate-determining barrier to rotation (TS7) about the 9,9′ bond is 48 kcal/mol relative to the P_xP_x minimum.

Conclusions

The synthesis of **1-Hex** demonstrates the utility of the biphenylating reagent **5** to prepare strained and hindered PAHs. In a single step, eight new aryl C−C bonds are formed with the introduction of ~80 kcal/mol of strain. The product, **1-Hex**, contains the only known example of a bond between two PAH gulfs. This bond is one of the more hindered single bonds in chemistry, and its energetic, structural, and dynamic consequences are extraordinary. Its adiabatic homolytic BDE is only 55% of biphenyl, but the bond has a normal length. The explanation, that strain is released slowly with extension, is revealed by calculations. VT NMR reveals two dynamic processes; analysis of the NMR spectra and calculations identify these processes as alkyl rotation and inversion of chirality. The full reaction coordinates for these processes are explored by DFT calculations and are rare examples of complex conformational behavior in PAHs, molecules that are often considered rigid. Neither observed process involves rotation about the hindered bond. The calculated reaction path for rotation about the central bond involves an unexpected slipped-parallel geometry; the simple notion of rotation about a torsion angle of the equilibrium structure fails completely.

Acknowledgment. This work was supported by the National Science Foundation (CHE-0449740; diffractometer, CHE-0226402; NMR spectrometers, CHE-0521191; mass spectrometer, CHE-0443647) and the NIH (MALDI-MS, P20-RR-016464). Computer time was provided in part by an allocation through the TeraGrid Advanced Support Program (NCSA CHE070052N).

Supporting Information Available: Synthetic procedures, NMR spectra, full thermal ellipsoid plots, and crystallographic information files for **1-Hex**•(benzene)$_{0.5}$, **1-Hex**•(benzene)$_2$, and **6**; computational details; and coordinates for all stationary points. This material is available free of charge via the Internet at http://pubs.acs.org.

JA803396N

(27) (a) Weinhold, F. *Angew. Chem., Int. Ed.* **2003**, *42*, 4188–4194. (b) Bickelhaupt, F. M.; Baerends, E. J. *Angew. Chem., Int. Ed.* **2003**, *42*, 4183–4188.
(28) Nori-shargha, D.; Asadzadeha, S.; Ghanizadehb, F.-R.; Deyhimic, F. *THEOCHEM* **2005**, *717*, 41–51.
(29) Rashidi-Ranjbar, P.; Sandström, J.; Schriver, G. W.; Wong, H. N. C. *Iran. J. Chem. Chem. Eng.* **1996**, *15*, 18–22.
(30) Schurig, V.; Reich, S. *Chirality* **1998**, *10*, 316–320.
(31) Grein, F. *J. Phys. Chem. A* **2002**, *106*, 3823–3827.
(32) Cioslowski, J.; Scott, A. P.; Radom, L. *Mol. Phys.* **1997**, *91*, 413–420.